

Frascati Physics Series

HEAVY QUARKS AND LEPTONS – San Juan, Puerto Rico, June 1 - June 5, 2004

The Case for a Super Neutrino Beam

Milind V. Diwan

Brookhaven National Laboratory

ABSTRACT

In this paper I will discuss how an intense beam of high energy neutrinos produced with conventional technology could be used to further our understanding of neutrino masses and mixings. I will describe the possibility of building such a beam at existing U.S. laboratories. Such a project couples naturally to a large (> 100 kT) multipurpose detector in a new deep underground laboratory. I will discuss the requirements for such a detector. Since the number of sites for both an accelerator laboratory and a deep laboratory are limited, I will discuss how the choice of baseline affects the physics sensitivities, the practical issues of beam construction, and event rates.

1 Introduction

In ¹⁾ we argued that an intense broadband muon neutrino beam and a large detector located more than 2000 km away from the source could be used to

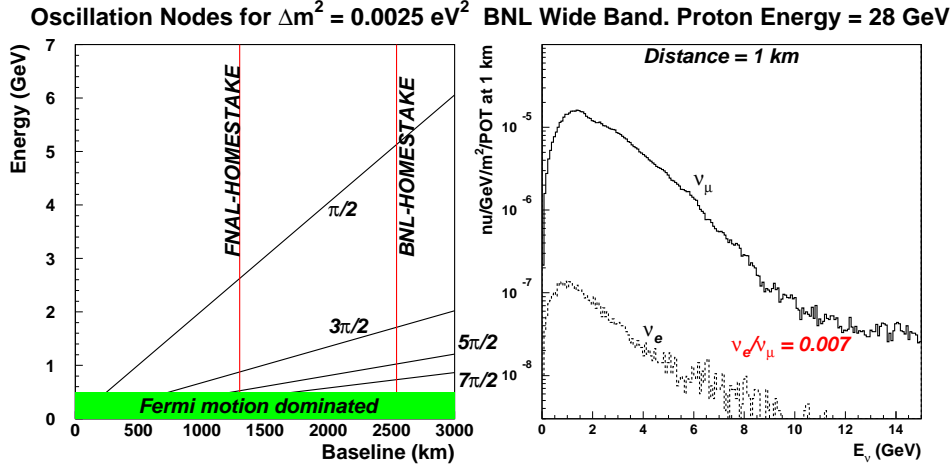


Figure 1: Nodes of oscillations for $\Delta m_{32}^2 = 0.0025 \text{ eV}^2$ in neutrino energy versus baseline (left). Possible baselines from Brookhaven National Laboratory (BNL) and Fermi National Laboratory (FNAL) to the Homestake underground site are indicated. They correspond to distances of $\sim 2540 \text{ km}$ and $\sim 1290 \text{ km}$, respectively. Right hand side shows the wide band neutrino spectrum from 28 GeV protons at a distance of 1 km from the target. The anti-neutrino spectrum looks similar, but has contamination from neutrinos.

perform precision measurements of neutrino properties such as the mass differences, the mass hierarchy, the mixing parameters, and CP violation in the neutrino sector. Using the currently deduced neutrino mass differences and mixing parameters ²⁾ and the same formalism as ¹⁾ we formulated several simple rules for such an experiment:

For precise measurements of Δm_{32}^2 and $\sin^2 2\theta_{23}$, it is desirable to observe a pattern of multiple nodes in the energy spectrum of muon neutrinos. Since the cross section, Fermi motion, and nuclear effects limit the resolution of muon neutrino interactions below $\sim 1 \text{ GeV}$, we need to utilize a wide band muon neutrino beam with energy range of 1-6 GeV and a distance of $\sim 2000 \text{ km}$ to observe 3 or more oscillation nodes. See Fig. 1.

The appearance spectrum of electron neutrinos from the conversion $\nu_\mu \rightarrow \nu_e$ contains information about $\sin^2 2\theta_{13}$, δ_{CP} , Δm_{21}^2 and the ordering of neutrino masses through the matter effect (i.e. $(m_1 < m_2 < m_3)$ versus $(m_3 < m_1 < m_2)$). We showed that the effects of the various parameters can be separated using the broad-band 1-6 GeV beam and the $\sim 2000 \text{ km}$ distance. The matter effect causes the conversion probability to rise with energy and is

mostly confined to energies > 3 GeV whereas the effects of δ_{CP} fall as $1/E$. We showed that this energy dependence can be used to measure the value of δ_{CP} and $\sin^2 2\theta_{13}$ without taking data with anti-neutrinos.

The additional contribution to the appearance event rate due to 3-generation CP violation in the neutrino sector is approximately proportional to: $\sin \delta_{CP} \sin 2\theta_{13} \times (\Delta m_{21}^2 L/4E_\nu)$. This contribution increases linearly with distance while the total flux falls as $1/L^2$ for a detector of a given size. The statistical sensitivity for the additional CP contribution, however, remains approximately independent of distance. It is therefore advantageous to perform the experiment with a very long (> 2000 km) baseline because then we can relax the requirements on systematic errors on the flux, the cross sections, the other oscillation parameters, and the calculation of the matter effect.

Because of the electron neutrino contamination background in a conventional accelerator neutrino beam the sensitivity to δ_{CP} will be limited to the parameter region $\sin^2 2\theta_{13} > 0.01$. The main CP-conserving contribution to the $\nu_\mu \rightarrow \nu_e$ signal is proportional to $\sin^2 2\theta_{13}$ in this region. The CP-violating term, on the other hand, is linear in $\sin 2\theta_{13}$. Therefore the fractional contribution due to the CP-violating term increases for small $\sin 2\theta_{13}$, although the total appearance signal decreases. The statistical sensitivity to the CP-violating term remains approximately independent of the value of $\sin^2 2\theta_{13}$ as long as backgrounds do not dominate the observed spectrum³⁾. When $\sin^2 2\theta_{13}$ is very small (< 0.002) this rule no longer holds because the signal is no longer dominated by the $\sin^2 2\theta_{13}$ term in the 3-generation formalism⁴⁾.

Current generation of accelerator experiments such as K2K⁵⁾, MINOS⁶⁾, or CNGS⁷⁾ focus on obtaining a definitive signature of muon neutrino oscillations at the first node ($\Delta m_{32}^2 L/4E \sim \pi/2$) for the atmospheric mass scale. Other recent proposed projects (JPARC-to-SK, NUMI-offaxis)^{8, 9)} also focus mainly on the first node, but propose to use an off-axis narrow band beam to lower the background in the search of $\nu_\mu \rightarrow \nu_e$ caused by a non-zero θ_{13} . The narrow band beam and limited statistics, however, do not allow measurement of the parameters in a definitive way. Proposed reactor disappearance searches, also at the first node for the atmospheric mass scale, are only sensitive to $\sin^2 2\theta_{13}$ ⁴⁾.

Thus, current and near term accelerator based experiments are focussed on the atmospheric mass scale. Experiments using astrophysical sources such as

solar neutrinos or atmospheric neutrinos are sensitive to either the solar or the atmospheric mass scale. The parameters are now known well enough ($\Delta m_{32}^2 \sim 0.0025 eV^2$ and $\Delta m_{21}^2 \sim 8 \times 10^{-5} eV^2$) ^{10, 11, 12)} that it is possible to design a qualitatively different experiment that will have good sensitivity to both mass scales. The CP contribution is dependent on both atmospheric and solar Δm^2 ; it is also likely that such an experiment is necessary to uncover any new physics in neutrino mixing or interactions with matter. A next generation accelerator experiment with well understood, pure beams, sufficiently long baseline, and low energy wide band beam (1-5 GeV) could fill this role.

In this paper we will discuss different options for the baseline. In ¹⁾ we demonstrated that for 3-generation mixing the CP parameters could be measured using neutrino data alone. Any additional information from anti-neutrino running therefore could make the measurements more precise as well as constrain contributions from new physics, in particular, new interactions in matter or new sources of CP violation in the neutrino sector. We will calculate the significance with which the neutrino mass and mixing parameters can be measured using both neutrino and anti-neutrino data and the implications for the determination of the mass hierarchy and demonstration of CP violation.

2 Accelerator and Detector Requirements

Previously we described the BNL Alternating Gradient Synchrotron (AGS) operating at 28 GeV upgraded to provide total proton beam power of 1 MW ¹³⁾ and a 500 kTon detector placed at the proposed national underground laboratory (NUSEL) ¹⁴⁾ in the Homestake mine in South Dakota. The main components of the accelerator upgrade at BNL are a new 1.2 GeV Superconducting LINAC to provide protons to the existing AGS, and new magnet power supplies to increase the ramp rate of the AGS magnetic field from about 0.5 Hz of today to 2.5 Hz. For 1 MW operation the protons from the accelerator will be delivered in pulses of 9×10^{13} protons at 2.5 Hz. We have determined that 2 MW operation of the AGS is also possible by further upgrading the synchrotron to 5 Hz repetition rate and with further modifications to the LINAC and the RF systems. The neutrino beam will be built with conventional horn focussed technology and a 200 m long pion decay tunnel.

High energy multi-MW proton beams are also under consideration at FNAL. The most ambitious plans ¹⁵⁾ call for a 8 GeV superconducting LINAC

that can provide 1.5×10^{14} H^- ions at 10 Hz corresponding to 2 MW of total beam power. Some of these 8 GeV ions could be injected into the main injector (MI) to provide 2 MW proton beam power at any energy between 40 and 120 GeV; for example, 40 GeV at 2 Hz or 120 GeV at 0.67 Hz. Such a plan allows much flexibility in the choice of proton energy for neutrino production. As Figure 1 shows for observing multiple oscillation nodes in muon neutrino oscillations it is necessary to have a wide band beam with energies from 1 to 5 GeV. Protons above ~ 20 GeV are needed to provide such a flux, clearly possible at either BNL or FNAL. For the purposes of the analysis in this paper we will assume that the spectrum from either the BNL or the FNAL beam will be the same. This will allow us a proper comparison of the physics issues regarding the baselines.

If a large detector facility (as a part of NUSEL) ^{16, 17, 18)} is located at Homestake (HS) the beam from BNL (FNAL) will have to traverse 2540km (1290km) through the earth. At BNL the beam would have to be built at an incline angle of about 11.3° . Current design for such a beam calls for the construction of a hill with a height of about 50 m ¹³⁾. Such a hill will have the proton target at the top of the hill and a 200 m long decay tunnel on the downslope. At FNAL the inclination will be about 5.7° . There is already experience at FNAL in building the NUMI beam ⁶⁾; this experience could be extended to build a new beam to HS. In either case, it is adequate to have a short decay tunnel (200 m) compared to the NUMI tunnel (750 m) to achieve the needed flux. The option of running with a narrow band beam using the off-axis technique ¹⁹⁾ could be preserved if the decay tunnel is made sufficiently wide. For example, a 4 m diameter tunnel could allow one to move and rotate the target and horn assembly so that a 1° off-axis beam could be sent to the far detector.

With 1 MW of beam, a baseline of 2540 km, and a 500kT detector we calculate that we would obtain ~ 60000 muon charged current and ~ 20000 neutral current events for 5×10^7 sec of running in the neutrino mode in the absence of oscillations. For the same running conditions in the anti-neutrino mode (with the horn current reversed) we calculate a total of ~ 19000 anti-muon charged current and ~ 7000 neutral current events; approximately 20% of the event rate in the anti-neutrino beam will be due to wrong-sign neutrino interactions. For the shorter baseline of 1290 km from FNAL to HS, the event

rates will be higher by a factor of $(2540/1290)^2$. For both neutrino and anti-neutrino running approximately $\sim 0.7\%$ of the charged current rate will be from electron charged current events which form a background to the $\nu_\mu \rightarrow \nu_e$ search. It will be desirable to obtain similar numbers of events in the anti-neutrino and the neutrino beam. Therefore, for the calculations in this paper we assume 1 MW operation for $5 \times 10^7 \text{sec}$ in the neutrino mode and 2 MW operation for $5 \times 10^7 \text{sec}$ in the anti-neutrino mode.

A large detector facility at NUSEL will most likely be used for a broad range of physics goals. Important considerations for such a detector are the fiducial mass, energy threshold, energy resolution, muon/electron discrimination, pattern recognition capability, time resolution, depth of the location, and the cost. Two classes of detectors are under consideration: water Cherenkov detector instrumented with photo-multiplier tubes and a liquid Argon based time projection chamber.

A water Cherenkov detector built in the same manner as the super-Kamiokande experiment (with 20 inch photo-multipliers placed on the inside detector surface covering approximately 40% of the total area ²⁰) can achieve the 500 kT mass. This could be done by simply scaling the super-Kamiokande detector to larger size or by building several detector modules ^{16, 17}). Such a detector placed underground at NUSEL could have a low energy threshold ($< 10 \text{ MeV}$), good energy resolution ($< 10\%$) for single particles, good muon/electron separation ($< 1\%$), and time resolution ($< \text{few ns}$). For the experiment we propose here it is important to obtain good energy resolution on the neutrino energy. This can be achieved in a water Cherenkov detector by separating quasi-elastic scattering events with well identified leptons in the final state from the rest of the charged current events. The fraction of quasi-elastic events in the total charged current rate with the spectrum used in this paper is about 23% for the neutrino beam and 39% for the anti-neutrino beam. Separation of quasi-elastic events from the charged current background is being used by the K2K experiment ⁵). Further work is needed to make this event reconstruction work at higher energies. The reconstruction algorithm could be enhanced by the addition of ring imaging techniques to the detector ²¹).

A number of proponents have argued that a liquid Argon time projection chamber (LARTPC) could be built with total mass approaching 100 kT ¹⁸). A fine grained detector such as this has much better resolution for separating

tracks. It is possible therefore to use a large fraction of the charged current cross section (rather than only the quasi-elastic events) for determining the neutrino energy spectrum. The LARTPC will also have much better particle identification capability. Therefore, a LARTPC with a smaller total fiducial mass of ~ 100 kT than the 500 kT assumed for the water Cherenkov tank is expected to have similar performance for the physics.

For the purposes of this paper we will assume the same detector performance as described in ¹⁾. For the physics sensitivity calculated in this paper we will assume 1 MW operation for $5 \times 10^7 \text{sec}$ in the neutrino mode and 2 MW operation for $5 \times 10^7 \text{sec}$ in the anti-neutrino mode. In both cases we will assume a detector fiducial mass of 500 kT. With the running times, the accelerator power level, and the detector mass fixed, we will consider two baselines: 1290 km (for FNAL to Homestake) and 2540 km (for BNL to Homestake) assuming that the detector is located at Homestake.

Lastly, we note that for this analysis the far detector could be at several comparable sites in the western US, notably WIPP or the Henderson mine in Colorado. While the detailed calculations change, the qualitative results are easily deduced from this work for other locations.

3 ν_μ disappearance

We propose to use clean single muon events ¹⁾ and calculate the neutrino energy from the energy and angle of these muons assuming they are all from quasi-elastic interactions. The expected spectrum is shown in Figure 2; the simulation includes effects of Fermi motion, detector resolution, and backgrounds from non-quasielastic events.

A great advantage of the very long baseline and multiple oscillation pattern in the spectrum is that the effect of systematic errors from flux normalization, background subtraction, and spectrum distortion due to nuclear effects or detector calibration can be small. Nevertheless, since the statistics and the size of the expected distortion of the spectrum are both large in the disappearance measurement, the final error on the precise determination of the parameters will most likely have significant contribution from systematic errors. In Figure 3 we show the 1 sigma resolutions that could be achieved on Δm_{32}^2 and $\sin^2 2\theta_{23}$. The black lines (labeled (1)) show the resolutions for purely statistical errors. For the red lines (labeled (2)) we have included a 5% bin-to-bin systematic un-

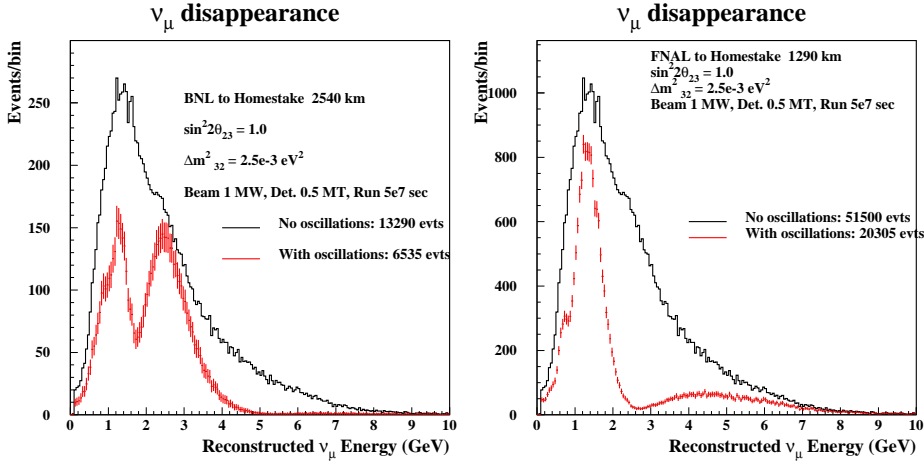


Figure 2: Simulated spectrum of detected muon neutrinos for 1 MW beam and 500 kT detector exposed for 5×10^7 sec. Left side is for baseline of 2540 km, right side for baseline of 1290 km. The oscillation parameters assumed are shown in the figure. Only clean single muon events are assumed to be used for this measurement (see text).

certainty in the spectrum shape and a 5% systematic uncertainty in the overall normalization. These uncertainties could include modeling of cross sections or knowledge of the background spectra. For the Δm_{32}^2 resolutions we also show the expected resolution for an additional systematic error of 1% on the global energy scale (blue line labeled (3)). This uncertainty for the Super Kamioka water Cherenkov detector is estimated to be 2.5% in the multi-GeV region²⁰).

Although the resolution on Δm_{32}^2 will be dominated by systematic errors for the proposed experimental arrangement, a measurement approaching 1–2% precision can clearly be made. On the other hand, the resolution on $\sin^2 2\theta_{23}$ is dominated by the statistical power at the first node. This results in a factor of ~ 2 better resolution with 1290 km than with 2540 km using the same sized detector.

Running in the anti-neutrino mode with 2 MW of beam power will yield approximately the same spectra and resolutions on Δm_{32}^2 and $\sin^2 2\theta_{23}$. By comparing the measurements with the results from neutrino running a test of CPT is possible. In such a comparison many systematic errors, such as the global energy scale, common to the neutrino and anti-neutrino data sets should cancel yielding a comparison with errors less than 1%.

Finally, we remark that it is important to make precision measurements

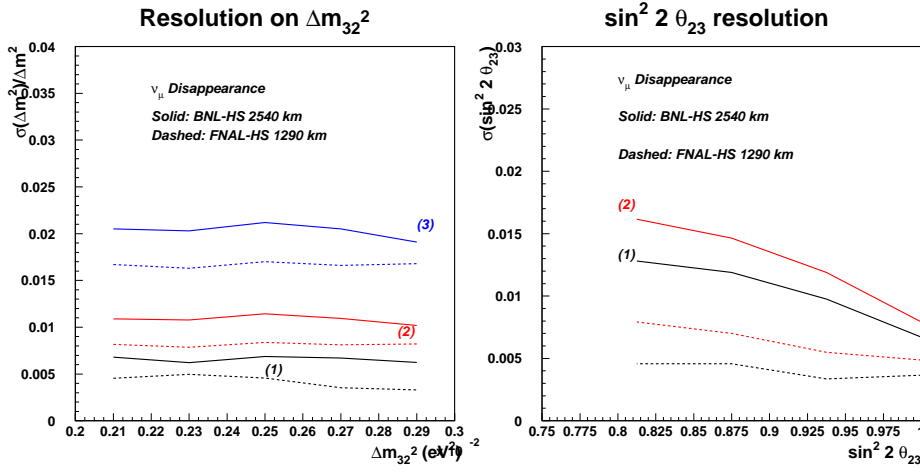


Figure 3: 1σ resolutions on Δm_{32}^2 (left) and $\sin^2 2\theta_{23}$ (right) expected after analysis of the oscillation spectra from Figure 2. The solid curves are for BNL-HS 2540 km baseline, and the dashed are for FNAL-HS 1290 km baseline. The curves labeled 1 and 2 correspond to statistics only and statistics and systematics, respectively (similarly for dashed curves of the same color). The curve labeled (3) on the left has an additional contribution of 1% systematic error on the global energy scale.

of both Δm_{32}^2 and $\sin^2 2\theta_{23}$ not only because they are fundamental parameters, but also because they are needed for interpreting the appearance ($\nu_\mu \rightarrow \nu_e$) result. Knowledge of both Δm_{21}^2 and Δm_{32}^2 are essential in fitting the shape of the appearance signal to extract other parameters. In addition, it will be very important to definitively understand if $\sin^2 2\theta_{23}$ is close to 1.0 or is < 1.0 . If $\sin^2 2\theta_{23} < 1.0$ then there will be an ambiguity in $\theta_{23} \rightarrow \pi/2 - \theta_{23}$. As we will describe below this ambiguity will affect the interpretation of the appearance spectrum.

4 ν_e appearance

Assuming a constant matter density, the oscillation of $\nu_\mu \rightarrow \nu_e$ in the Earth for 3-generation mixing is described approximately by the following equation (22)

$$\begin{aligned}
 P(\nu_\mu \rightarrow \nu_e) \approx & \sin^2 \theta_{23} \frac{\sin^2 2\theta_{13}}{(\hat{A} - 1)^2} \sin^2((\hat{A} - 1)\Delta) \\
 & + \alpha \frac{\sin \delta_{CP} \cos \theta_{13} \sin 2\theta_{12} \sin 2\theta_{13} \sin 2\theta_{23}}{\hat{A}(1 - \hat{A})} \sin(\Delta) \sin(\hat{A}\Delta) \sin((1 - \hat{A})\Delta)
 \end{aligned}$$

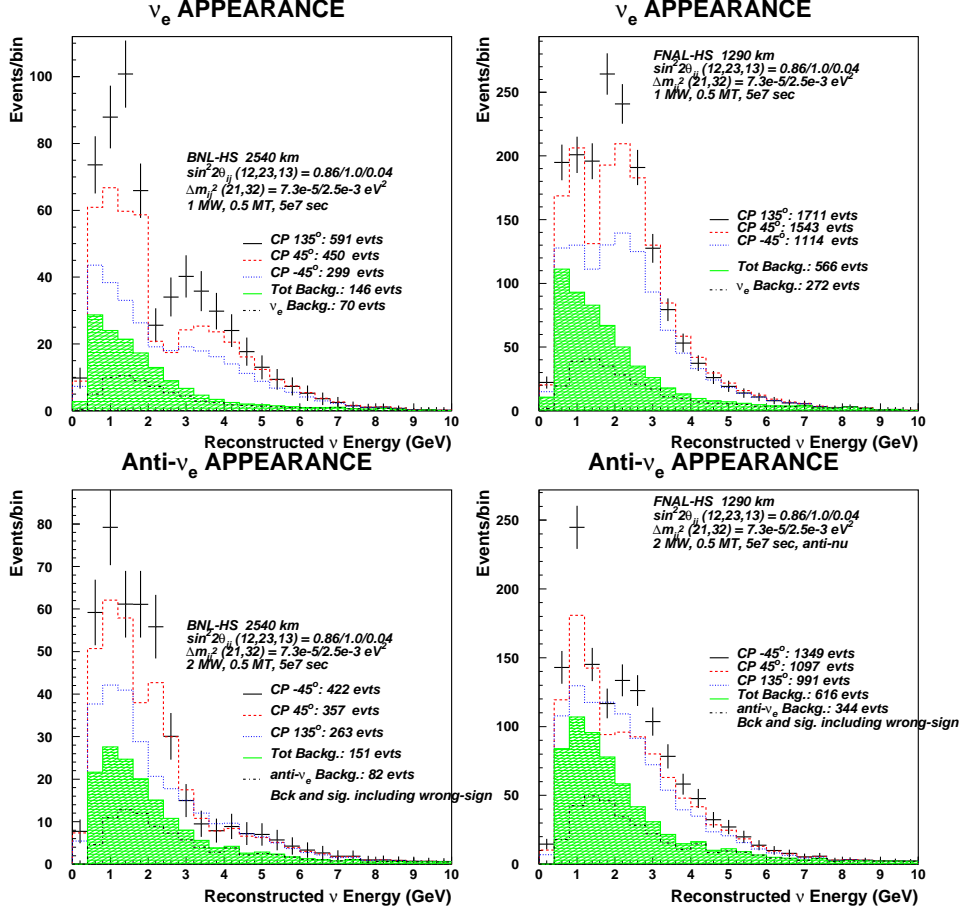


Figure 4: Simulation of detected electron neutrino (top plots) and anti-neutrino (bottom plots) spectrum (left for BNL-HS 2540km, right for FNAL-HS 1290 km) for 3 values of the CP parameter δ_{CP} , 135° , 45° , and -45° , including background contamination. Obviously, the dependence of event rate on the CP phase has the opposite order for neutrinos and anti-neutrinos. The hatched histogram shows the total background. The ν_e beam background is also shown. The other assumed mixing parameters and running conditions are shown in the figure. These spectra are for the regular mass hierarchy (RO).

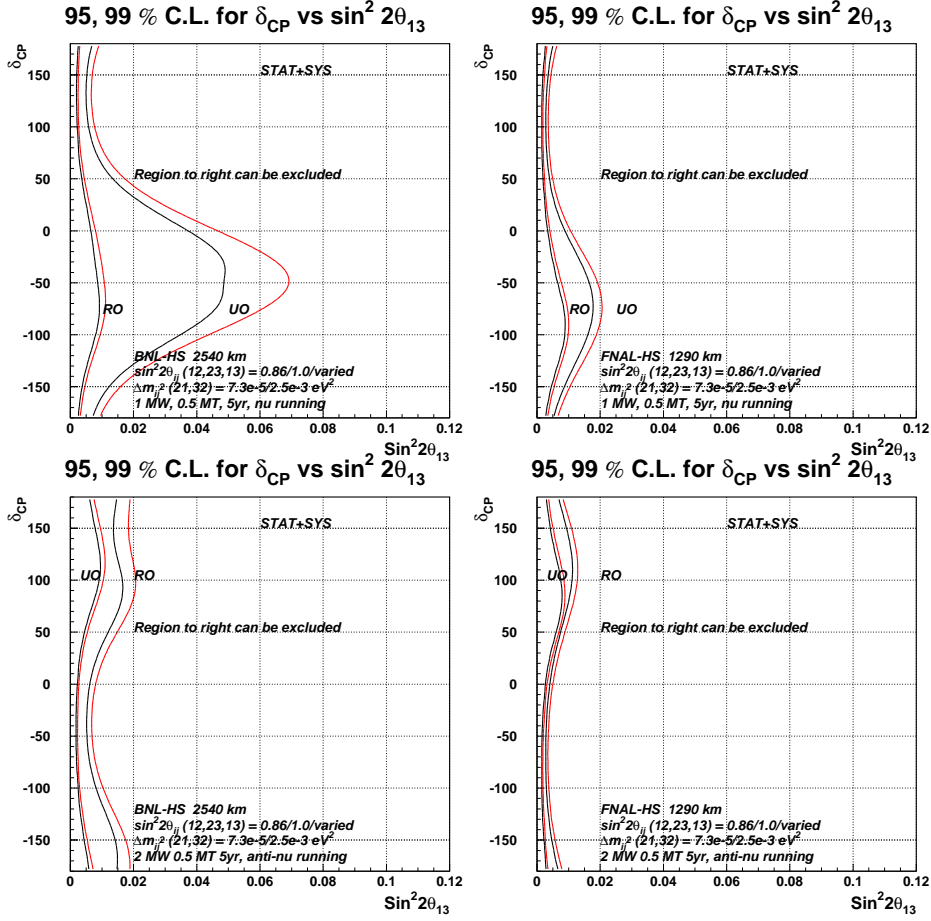


Figure 5: Expected limit on $\sin^2 2\theta_{13}$ as a function of δ_{CP} for BNL-HS neutrino running only (top left), FNAL-HS neutrino running only (top right), BNL-HS anti-neutrino running only (bottom left), FNAL-HS anti-neutrino running only (bottom right).

$$\begin{aligned}
& +\alpha \frac{\cos \delta_{CP} \cos \theta_{13} \sin 2\theta_{12} \sin 2\theta_{13} \sin 2\theta_{23}}{\hat{A}(1-\hat{A})} \cos(\Delta) \sin(\hat{A}\Delta) \sin((1-\hat{A})\Delta) \\
& +\alpha^2 \frac{\cos^2 \theta_{23} \sin^2 2\theta_{12}}{\hat{A}^2} \sin^2(\hat{A}\Delta)
\end{aligned} \tag{1}$$

where $\alpha = \Delta m_{21}^2/\Delta m_{31}^2$, $\Delta = \Delta m_{31}^2 L/4E$, $\hat{A} = 2VE/\Delta m_{31}^2$, $V = \sqrt{2}G_F n_e$. n_e is the density of electrons in the Earth. Recall that $\Delta m_{31}^2 = \Delta m_{32}^2 + \Delta m_{21}^2$. Also notice that $\hat{A}\Delta = LG_F n_e/\sqrt{2}$ is sensitive to the sign of Δm_{31}^2 . For anti-neutrinos, the second term in Equation 1 has the opposite sign. It is proportional to the following CP violating quantity.

$$J_{CP} \equiv \sin \theta_{12} \sin \theta_{23} \sin \theta_{13} \cos \theta_{12} \cos \theta_{23} \cos^2 \theta_{13} \sin \delta_{CP} \tag{2}$$

Equation 1 is an expansion in powers of α . The approximation becomes inaccurate for $\Delta m_{32}^2 L/4E > \pi/2$ as well as $\alpha \sim 1$. For the actual results we have used the exact numerical calculation, accurate to all orders. Nevertheless, the approximate formula is useful for understanding important features of the appearance probability: 1) the first 3 terms in the equation control the matter induced enhancement for regular mass ordering (RO) ($m_1 < m_2 < m_3$) or suppression for the unnatural or reversed mass ordering (UO) ($m_3 < m_1 < m_2$) of the oscillation probability above 3 GeV; 2) the second and third terms control the sensitivity to CP in the intermediate 1 to 3 GeV range; and 3) the last term controls the sensitivity to Δm_{21}^2 at low energies.

The ν_e signal will consist of clean, single electron events (single showering rings in a water Cherenkov detector) that result mostly from the quasi-elastic reaction $\nu_e + n \rightarrow e^- + p$. The main backgrounds will be from the electron neutrino contamination in the beam and reactions that have a π^0 in the final state. The π^0 background will depend on how well the detector can distinguish events with single electron induced and two photon induced electromagnetic showers. Assuming the same detector performance as in ¹⁾ we calculate the expected electron neutrino and anti-neutrino spectra shown in Figure 4. These spectra were calculated for the parameters indicated in the figures for the regular mass ordering (RO). For the reversed mass ordering (UO) the anti-neutrino (neutrino) spectrum will (not) have the large matter enhancement at higher energies. The dependence of the total event rate on the CP phase parameter is the same for RO and UO in either running mode.

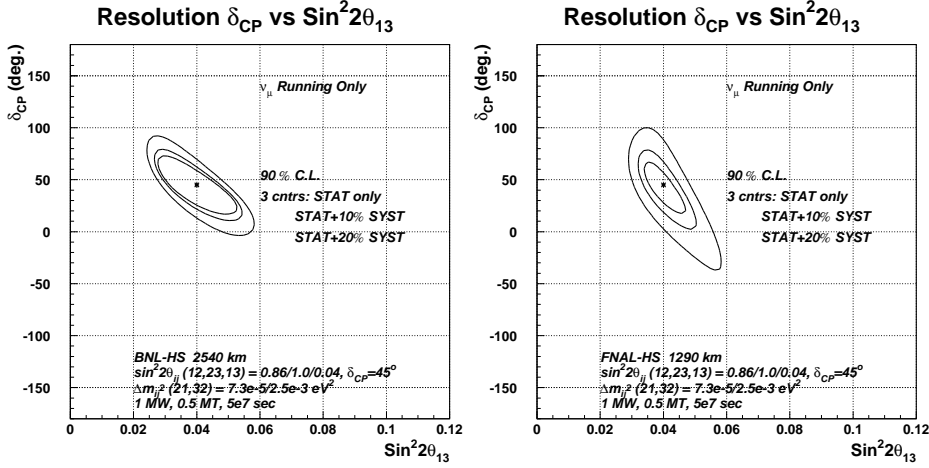


Figure 6: 90% confidence level error contours in $\sin^2 2\theta_{13}$ versus δ_{CP} for statistical and systematic errors with neutrino data alone. Left is for BNL-HS and right is for FNAL-HS. The test point used here is $\sin^2 2\theta_{13} = 0.04$ and $\delta_{CP} = 45^\circ$. $\Delta m_{32}^2 = 0.0025 \text{ eV}^2$, and $\Delta m_{21}^2 = 7.3 \times 10^{-5} \text{ eV}^2$. The values of $\sin^2 2\theta_{12}$ and $\sin^2 2\theta_{23}$ are set to 0.86, 1.0, respectively.

4.1 θ_{13} and δ_{CP} phase

If there is no excess of electron events observed then we can set a limit on the value of $\sin^2 2\theta_{13}$ as a function of δ_{CP} . Such 95 and 99% C.L. sensitivity limits are shown in Figure 5. These set of plots illustrate various considerations that must be evaluated for the very long baseline project. After running initially in the neutrino mode with 1 MW of beam power, if an excess signal is found then a measurement of δ_{CP} versus $\sin^2 2\theta_{13}$ can be made as shown in Figure 6, at the same time the mass hierarchy is determined from the strength of the signal in the higher energy region. If there is no signal in the neutrino mode then either θ_{13} is too small for the regular mass hierarchy (RO) or the mass hierarchy is reversed (UO) and parameters are in the “unlucky” region ($-140^\circ < \delta_{CP} < 30^\circ$). For the shorter baseline of 1290 km, the θ_{13} sensitivity for the reversed hierarchy is not reduced as much as for 2540 km because both the CP-sensitivity and the matter effect are weaker. Although this yields a better limit for $\sin^2 2\theta_{13}$ in the absence of signal, it affects the precision on δ_{CP} and the determination of the mass hierarchy.

If there is no signal in the neutrino mode, we will run in the anti-neutrino mode to cover the “unlucky” parameter space for the appearance signal. A

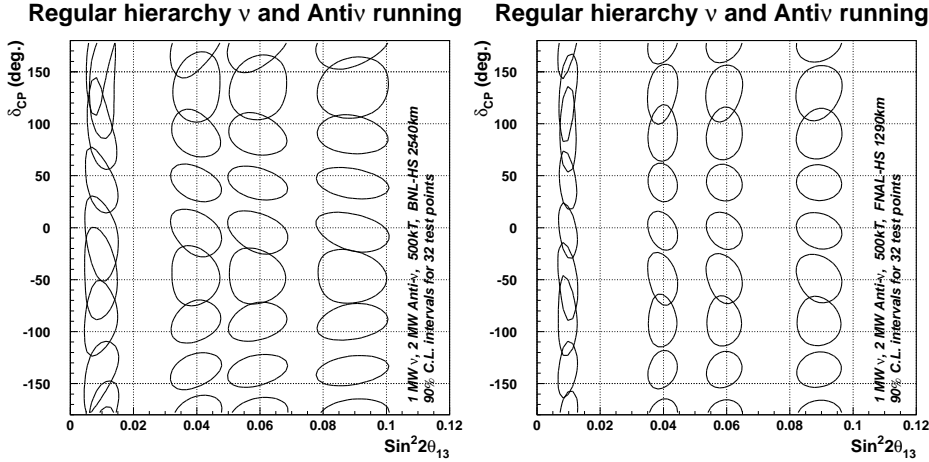


Figure 7: 90% confidence level error contours in $\sin^2 2\theta_{13}$ versus δ_{CP} for statistical and systematic errors for 32 test points. This simulation is for combining both neutrino and anti-neutrino data. Left is for BNL-HS and right is for FNAL-HS. We assume 10% systematic errors for this plot.

combination of neutrino and anti-neutrino running will yield a stringent limit approaching $\sin^2 2\theta_{13} \sim 0.003$ independent of the value of δ_{CP} . The simulation results shown here include wrong sign contamination in both the background and signal for anti-neutrinos. Interestingly, since more than 20% of the event rate in the anti-neutrino case actually arises from the neutrino contamination, the $\sin^2 2\theta_{13}$ limit in the anti-neutrino case exhibits less dependence on δ_{CP} and the mass hierarchy. If there is a signal in the neutrino mode, we will get the first measurement of δ_{CP} from neutrino data alone in the 3-generation model, but it will still be important to run in the anti-neutrino mode for better precision, over-constraints on the 3-generation model, and search for possible new physics either in the mixing or in the interactions of neutrinos.

In Figure 6 we show the 90% confidence level interval in the δ_{CP} versus $\sin^2 2\theta_{13}$ plane from neutrino running alone for the two baselines. We have chosen the point $\delta_{CP} = 45^\circ$ and $\sin^2 2\theta_{13} = 0.04$ as an example. At this test point for the regular mass hierarchy, the resolution on δ_{CP} is $\sim \pm 20^\circ$. The mass hierarchy is also resolved at > 5 sigma because of the large enhancement of the spectrum at higher energies. As we pointed out in the introduction, the resolution on the CP phase is approximately independent of the baseline. The major difference between the 1290 and 2540 km baselines is that the shorter baseline has higher correlation between the parameters, δ_{CP} and $\sin^2 2\theta_{13}$, has

better resolution on $\sin^2 2\theta_{13}$, and has worse sensitivity to systematic errors on the background and the spectrum shape. If the systematic errors exceed 10%, the shorter baseline will most likely have worse performance for measuring the CP parameter.

The sensitivity to systematic errors and the dependence on the mass hierarchy can be relieved by using data from both neutrino and anti-neutrino running. Figure 7 shows the 90% confidence level interval for 32 test points in the δ_{CP} and $\sin^2 2\theta_{13}$ plane after both neutrino and anti-neutrino data. A number of observations can be made: Figure 7 is for the regular mass hierarchy. The plot for the reversed mass hierarchy is similar. After both neutrino and anti-neutrino data the hierarchy will be resolved to more than 10 sigma (somewhat less significance for the shorter baseline) for $\sin^2 2\theta_{13}$ as small as 0.01. The resolution on δ_{CP} is seen to be approximately independent of $\sin^2 2\theta_{13}$ for $\sin^2 2\theta_{13} > 0.01$. When $\sin^2 2\theta_{13}$ is so small that the background becomes dominant, the δ_{CP} resolution becomes poor. The resolution on δ_{CP} is seen to be approximately the same for 2540 and 1290 km, except for small $\sin^2 2\theta_{13}$ where large statistics at 1290 km are seen to overcome the background. The resolution on $\sin^2 2\theta_{13}$ is, however, better for the shorter baseline because the sensitivity comes from the first node of oscillations which has much higher statistics at the shorter baseline.

4.2 Correlations with other parameters

The measurement of δ_{CP} using a wide band beam and multiple oscillation nodes is largely free of ambiguities and correlations²³⁾. The $\delta_{CP} \rightarrow \pi - \delta_{CP}$ ambiguity is resolved by the detection of multiple nodes including the effects of the $\cos \delta_{CP}$ term. The mass hierarchy is resolved because it has a strong energy dependence obvious in the shape of the spectrum.

The remaining main sources of correlations are the uncertainty on Δm_{21}^2 and $\sin^2 2\theta_{23}$. The CP terms in Equation 1 are linear in Δm_{21}^2 , therefore the systematic uncertainty on the event rate at the second oscillation maximum will be $< 10\%$, which is the uncertainty on Δm_{21}^2 from solar neutrino and KAMLAND experiments. As discussed above, this level of uncertainty will not affect the CP measurement for the longer baseline of 2540 km, but could be important for the shorter baseline of 1290 km.

An examination of Equation 1 shows that the knowledge of θ_{23} affects the

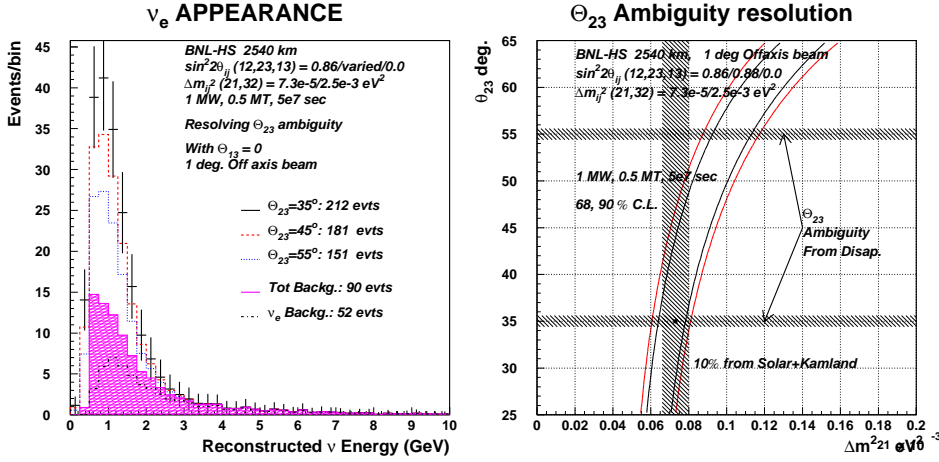


Figure 8: Expected spectrum of electron neutrinos (left) for $\theta_{13} = 0$ and other assumed parameters indicated in the figure. The right hand side shows the resolution of the $\theta_{23} \rightarrow \pi/2 - \theta_{23}$ ambiguity using the measurement of $\sin^2 2\theta_{23}$ from disappearance and assuming a 10% measurement of Δm_{21}^2 from KAMLAND. The area between the curves is allowed by the appearance spectrum (left) for $\theta_{23} = 35^\circ$.

first (Δm_{31}^2 dominated) and the last (Δm_{21}^2 dominated) terms as $\sin^2 \theta_{23}$ and $\cos^2 \theta_{23}$, respectively. The first term is responsible for the matter enhanced (or suppressed) appearance at high energies and the last term is responsible for appearance at low energies. Current knowledge of θ_{23} from atmospheric neutrinos¹⁰⁾ is rather poor: $35 < \theta_{23} < 55^\circ$. A precise determination of $\sin^2 2\theta_{23}$ using the muon disappearance spectrum is, therefore, essential for proper interpretation of the appearance signal. A 1% determination of $\sin^2 2\theta_{23}$ (Figure 3) leads to an uncertainty of $\sim 10\%$ on the appearance event rates if $\theta_{23} \sim 45^\circ$ and $\sim 2\%$ if $\theta_{23} \sim 35^\circ$. If $\theta_{23} \sim 35^\circ$ then there is also the additional ambiguity of $\theta_{23} \rightarrow \pi/2 - \theta_{23}$. Because of the strong energy dependence at low and high energies the ambiguity as well as the uncertainty should not affect the interpretation of the neutrino data in the case of the longer 2540km baseline. Uncertainties on both Δm_{21}^2 and θ_{23} affect the neutrino and anti-neutrino appearance spectra in the same manner, therefore after both data sets are acquired these systematic errors are expected to have little effect on establishing CP violation in neutrinos, but may affect the determination of parameters in the case of the shorter baseline.

It is important to understand the physics case for the super-beam if

$\sin^2 2\theta_{13}$ is so small that the background prevents us from detecting a signal. In this case, both the mass hierarchy through the matter effect and the CP phase measurement are not accessible for any baseline. However, the $\nu_\mu \rightarrow \nu_e$ conversion signature still could be accessible for the longer baseline of 2540 km because of the last term in Equation 1. This term depends on the “solar” Δm_{21}^2 as well as $\sin^2 2\theta_{12}$ and $\cos^2 \theta_{23}$. For the current value of the solar parameters ~ 100 events could be expected over a similar background. This is shown in Figure 8 where we have used a 1 degree off-axis neutrino spectrum to reduce the background level at low energies. For this calculation we have used $\sin^2 2\theta_{23} = 1.0$ and $\sin^2 2\theta_{23} = 0.88$ as test points. We assume that $\sin^2 2\theta_{23}$ will be measured with $\sim 1.5\%$ precision in disappearance. In the case of $\sin^2 2\theta_{23} = 0.88$, we are lead to an ambiguity in θ_{23} of $35^\circ \pm 0.6^\circ \rightarrow 55^\circ \pm 0.6^\circ$. This ambiguity is clearly distinguished at several sigma in the case of the 2540 km baseline as shown in the right hand side of Figure 8. The ambiguity resolution is accomplished by comparing the result of appearance with the result of $\bar{\nu}_e$ disappearance from solar and KAMLAND measurements. For Figure 8 we assume that Δm_{21}^2 will be determined to $\sim 10\%$. This comparison of appearance and disappearance experiment could also be important for uncovering new physics in this sector.

5 Conclusion

We have studied various possible measurements using a powerful neutrino beam, using a MW-class proton source located either at BNL or FNAL, to a large capable detector with fiducial mass in excess of 100kT over a distance ~ 2000 km. For our study here, we chose the distances of 1290 and 2540km because they correspond to the distances from FNAL and BNL to Homestake in South Dakota, one of the possible sites for a large detector. Nevertheless, our results are applicable to any other site in the U.S. at a comparable distance from an accelerator laboratory. Qualitatively, this project is motivated by the need to perform an experiment that is sensitive to both the atmospheric ($\Delta m_{32}^2 \sim 0.0025 eV^2$) and the solar ($\Delta m_{21}^2 \sim 8 \times 10^{-5} eV^2$) oscillation scales and to obtain an oscillatory pattern in the energy spectrum of muon neutrinos. The detector requirements for such an experiment – both in size and performance – are well-matched to other important goals in particles physics, such as detection of proton decay and astrophysical neutrinos. Therefore the potential physics impact is very broad for particle and astrophysics.

In this paper we have shown that very precise measurements of Δm_{32}^2 and $\sin^2 2\theta_{23}$ can be made using the observation of the oscillatory spectrum of muon neutrinos at either 1290 or 2540 km. For these precise measurements the shorter baseline has an advantage because of the increased statistical power, however it is very likely that the measurements will be systematics dominated to about 1% for either distance. We have also shown that very good bounds on $\sin^2 2\theta_{13}$ can be obtained from both baselines using the appearance of electron neutrinos. The electron event rate at shorter baseline has smaller matter effect and smaller dependence on the CP phase. Therefore, the θ_{13} bound using the neutrino data alone from the shorter baseline will have less dependence on the CP phase and the mass hierarchy. When both neutrino and anti-neutrino data are combined the δ_{CP} and mass hierarchy dependence is eliminated for both baselines, and the θ_{13} bound from either baseline will likely be dominated by the knowledge of backgrounds. The limit on $\sin^2 2\theta_{13}$ could reach ~ 0.003 if total number of background events can be controlled to about twice the expectation from the electron neutrino contamination in the beam ($\sim 0.7\%$).

If a signal is found for electron appearance then the value of the CP phase can be determined from the shape of the spectrum using neutrino data alone for either baseline. A more precise measurement of the CP phase and further constraint on the 3-generation model can be made by additional running in the anti-neutrino mode. There are some advantages for having the longer 2540 km baseline for the CP measurement. The matter effect is much larger and therefore the mass hierarchy can be resolved with greater confidence. The effect of δ_{CP} on the spectrum is also much larger for the longer baseline. This allows extraction of the parameter δ_{CP} without relying on very precise determination of the spectrum shape. The systematics of the spectrum shape are dependent not only on the knowledge of the beam, but also on other neutrino parameters such as Δm_{31}^2 , θ_{23} , Δm_{21}^2 , and θ_{12} . These parameters must be obtained from solar and reactor experiments, and from the muon neutrino disappearance analysis. A 10% systematic uncertainty on the backgrounds and the shape of the spectrum is tolerable for the 2540 km baseline, whereas the uncertainty needs to be smaller for the shorter baseline experiment. In addition, the longer baseline allows detection of the appearance of electron neutrinos even if θ_{13} is too small, through the effect of Δm_{21}^2 alone. This observation can also help separate the $\theta_{23} \rightarrow \pi/2 - \theta_{23}$ ambiguity if needed.

Despite the small, but significant differences between the two possible baselines, we conclude that an experiment using a beam from either FNAL or BNL to a large next generation multipurpose detector is very important for particle physics and could lead to major advances in our understanding of neutrino phenomena. It is important to recognize that the detector meant for such an experiment needs to be highly capable in terms of pattern recognition and energy resolution. If such a detector is located in a deep low background environment, it has broad applications in searching for nucleon decay and astrophysical neutrino sources. There are many advantages if both beams can be built and sent to the same detector. The correlation between parameters and the size of the matter effect are different for the two baselines. It is possible that by combining the results from the two baselines all dependence on external parameters could be eliminated, and the neutrino sector much better constrained. The requirement on total running time could also be reduced.

This work was supported by DOE grant DE-AC02-98CH10886. I also want to thank the Aspen Center for Physics where much of the writing of this paper took place.

References

1. “Very Long Baseline Neutrino Oscillation Experiment for Precise Measurements of Mixing Parameters and CP Violating Effects”, M. V. Diwan, *et al.*, **PRD** **68** (2003) 012002.
2. PDG, Phys. Rev. **D66**, 010001 (2002), p. 281.
3. W. Marciano, hep-ph/0108181, 22 Aug. 2001.
4. Stephen Parke, Talk in the HQL04 conference, Puerto Rico, June 1-June5, 2004.
5. S. H. Ahn et al., Phys. Lett. **B** **511** 178 (2001).
6. Numi MINOS project at Fermi National Accelerator Laboratory, <http://www-numi.fnal.gov/>
7. The CERN Neutrino beam to Gran Sasso (Conceptual Technical Design), Ed. K. Elsener, CERN 98-02, INFN/AE-98/05, <http://proj-cnsgs.web.cern.ch/proj-cnsgs/>

8. The JHF-Kamioka neutrino project, Y. Itow et al., arXiv:hep-ex/0106019, June 2001.
9. Letter of Intent to build an Off-axis Detector to study neutrino oscillations with the NuMI Neutrino Beam, D. Ayres *et al.*, hep-ex/0210005.
10. Y. Fukuda et al., Phys. Rev. Lett. **81**, 1562 (1998); S. Fukuda et al., Phys. Rev. Lett. **86** 5656, 2001; E.W. Beier, Phys. Lett. **B283**, 446 (1992); T. Kajita and Y. Totsuka, Rev. Mod. Phys. **73**, 85 (2001).
11. K. Eguchi, *et. al.*, Phys. Rev. Lett. **90**, 021802 (2003). hep-ex/0212021.
12. Q. R. Ahmad et al., Phys. Rev. Lett. **87** 071301 (2001). S. Fukuda et al., Phys. Rev. Lett., **86** 5651 (2001).
13. J. Alessi *et al.*, AGS Super Neutrino Beam Facility, Accelerator and Target system Design, BNL-71228-2003-IR. April 15, 2003. <http://nwg.phy.bnl.gov/>
14. Neutrinos and Beyond: New Windows on Nature, Neutrino Facilities Assessment Committee, National Research Council, (2003), ISBN-0-309-08716-3, <http://www.nap.edu/catalog/10583.html>.
15. R. Alber, et al., Accelerator Proton Driver Study Group FNAL-TM-2136, FNAL-TM-2169. <http://www-bd.fnal.gov/pdriver/>
16. Megaton Modular Multi-Purpose Neutrino detector, 3M collaboration, <http://www.hep.upenn.edu/Homestake>
17. Physics Potential and Feasibility of UNO, UNO collaboration, June 2001, Stony Brook University, SBHEP01-03.
18. D.B. Cline, F. Segiampietri, J.G. Learned, K.T. McDonald, *LANNDD, A Massive Liquid Argon Detector for Proton Decay, Supernova and Solar neutrino Studies, and a Neutrino Factory Detector* May 24, 2001, astro-ph/0105442; F. Arneodo et al., Nucl. Instrum. Meth. **A471** 272-275 (2000).
19. The “off-axis” neutrino beam was first proposed by the E889 Collaboration, Physics Design Report, BNL No. 52459, April, 1995. <http://minos.phy.bnl.gov/nwg/papers/E889>.

20. S. Fukuda et al., Nucl. Instrm. Meth. A **501**, (2003) 418-462.
21. P. Antonioli et al., Nuclear Instrm. Methods **A433** 104-120, (1999).
22. M. Freund, Phys.Rev. D64 (2001) 053003; M. Freund, P. Huber, M. Lindner, Nucl.Phys. B615 (2001) 331-357;
23. V.D. Barger, S. Geer, R. Raja, K. Whisnant, Phys. Rev. D63: 113011 (2001); V. Barger et al., hep-ph/0103052; P. Huber, M. Lindner, W. Winter, Nucl. Phys. B645, 3 (2002); V. Barger, D. Marfatia, K. Whisnant, Phys. Rev. D65: 073023 (2002).